In-vivo diffusing-wave-spectroscopy measurements of the ocular fundus

L. Rovati, S. Cattini, N. Zambelli

Dipartimento di Ingegneria dell'Informazione, Università degli Studi di Modena e Reggio Emilia, Via Vignolese 905/b, 41100 Modena, Italy
rovati.luigi@unimo.it

F. Viola and G. Staurenghi

Clinica Oculistica, Ospedale Luigi Sacco, Università di Milano, via G..B. Grassi, 74 20100 Milan, Italy
giovanni.staurenghi@unimi.it

Abstract: We present what is to our knowledge the first observation of a diffusing-wave-spectroscopy signal recorded in-vivo on the ocular fundus. A modified ophthalmic microscope was developed which can acquire diffusing-wave-spectroscopy signal from the eye fundus. The diffusing-wave-spectroscopy signal was recorded in-vivo on a rabbit eye during transpupillary thermotherapy. Experimental results show the ability of the system to detect motion of the scattering sites in the ocular fundus layers during laser thermal heating.

OCIS codes: (120.3890) Medical optics instrumentation; (170.4470) Ophthalmology; (120.5820) Scattering measurements; (170.6510) Spectroscopy, tissue diagnostics; (170.1470) Blood/tissue constituent monitoring

References and Links

1. D.J. Pine, D.A. Weitz, P.M. Chaikin, and E. Herbolzheimer, "Diffusing-Wave Spectroscopy," Phys. Rev. Lett. **60**, ll34-ll37 (1988).
2. D.A. Boas, M.A. O'Leary, B. Chance and A.G. Yodh, "Scattering of Diffuse Photon Density Waves by Spherical Inhomogeneties within Turbid Media: Analytic Solution and Applications," Proc. Nail. Acad. Sci. USA **91**, 4887-4891 (1994).
3. D.A. Boas, L.E. Campbell and A.G. Yodh, "Scattering and Imaging with Diffusing Temporal Field Correlation," Phys. Rev. Lett. **75**, 1855-1858 (1995).
4. F.C. MacKintosh and S. John, "Diffusing-wave spectroscopy and multiple scattering of light in correlated random media," Phys. Rev. B **40**, 2382-2406 (1989).
5. M. Hammer, A. Roggan, D. Scweitzer and G. Müller, "Optical properties of ocular fundus tissue-an in vitro study using the double-integrating-sphere technique and inverse Monte Carlo simulation," Phys. Med. Biol. **40**, 963-978 (1995).
6. D.A. Weitz and D.J. Pine, *Dynamic Light Scattering: The Method and Some Applications* (Claredon Press, Oxford,1993).
7. A.D. Gopal and D.J. Durian, "Shear-Induced "Melting" of an Aqueous Foam," J. Colloid Interface Sci. **213**, 169–178 (1999).
8. P.A. Lemieux, M. U. Vera and D. J. Durian, "Diffusing-light spectroscopies beyond the diffusion limit: The role of ballistic transport and anisotropic scattering," Phys. Rev. E **57**, 4498-4515 (1998).
9. A. Kienle, "Non-invasive determination of muscle blood flow in the extremities from laser Doppler spectra," Phys. Med. Biol. **46**, 1231–1244 (2001).
10. R. Cubeddu, A. Pifferi, P. Taroni, A. Torricelli and G. Valentini, " Compact tissue oximeter based on dual-wavelength multichannel time-resolved reflectance," App. Opt. **38**, 3670-3680 (1999).
11. L. Rovati, F. Fankhauser II, and J. Ricka, "Design and performance of a new ophthalmic instrument for dynamic light scattering in the human eye," Rev. Sci. Instrum. **67**, 2615-2620 (1996).
12. R.S. Newsom, J.C. McAlister, M. Saeed and J.D. McHugh, "Transpupillary thermotherapy (TTT) for the treatment of choroidal neovascularisation," Br J Ophthalmol. **85**, 173–178 (2001).
13. W.S. Weinberg, R. Birngruber and B. Lorenz, "The Change in Light Reflection of the Retina During Therapeutic Laser-Photocoagulation determined by histological examination," IEEE J. Quantum Electron. **QE-20**, 1481-1489 (1984).

#77218 - $15.00 USD Received 17 November 2006; revised 17 January 2007; accepted 7 March 2007

14. S.E. Skipetrov and I.V. Meglinski, "Diffusing-wave spectroscopy in randomly inhomogeneous media with spatially localized scatterer flows," J. Exp. Theor. Phys. **86**, 661-665 (1998).
15. F. Scheffold, S. E. Skipetrov, S. Romer and P. Schurtenberger, "Diffusing-wave spectroscopy of nonergodic media," Physical Review E **63**, 0614041-06140411 (2001).
16. G. Maret and P.E. Wolf, "Multiple light scattering from disordered media. The effect of brownian motion of scatterers," Z Phys. B **65**, 409-413 (1987).
17. S.E. Skinpetrov and R. Maynard, "Dynamic multiple scattering of light in multilayer turbid media," Phys. Lett. A **217**,181-185 (1996).
18. J. Kandulla, H. Elsner, R. Birngruber and R. Brinkmann, "Noninvasive optoacoustic online retinal temperature determination during continuous-wave laser irradiation," J. Biomed. Opt. **11**, 0411111-04111113 (2006).
19. M.A. Mainster and E. Reichel, "Transpupillary thermotherapy for age-related macular degeneration: long-pulse photocoagulation, apoptosis, and heat shock proteins," Ophthalmic Surg. Lasers **31**, 359-73 (2000).
20. R.W. Flower, C. Von Kerczek, L. Zhu, A. Ernest, C. Eggleton and L.D.T. Topoleski, "Theoretical investigation of the role of choriocapillaris blood flow in treatment of subfoveal choroidal neovascularization associated with age-related macular degeneration," Am. J. Opthamol. **132**, 85-93 (2001).
21. L.M. Parver C.R. Auker and D.O. Carpenter, "Choroidal blood flow as a heat dissipating mechanism in macula," Am J Ophthalmol **89**, 641-646 (1980).
22. L.M. Parver C.R. Auker and D.O. Carpenter, "The stabilizing effect of the choroidal circulation on the temperature environment of the macula," Retina **2**, 117-120 (1982).
23. L.M. Parver C.R. Auker, D.O. Carpenter and I. Doyle, "Choroidal blood flow, II: reflexive control in the monkey," Arch Ophthalmol **100**, 1327-1330 (1982).
24. L.M. Parver C.R. Auker and D.O. Carpenter, ""Choroidal blood flow, III: : reflexive control in human eye," Arch Ophthalmol **101**, 1604-1606 (1983).
25. M. Bonaiuti, C. Riva and L. Rovati, "Optic nerve blood flow response to flicker can be described by a second order linear system model" in *Proceeding ARVO* **47** (Invest Opthalmol Vis Sci, Ft. Lauderdale, Florida, 2006), p. 493.
26. T. Nagaoka, and A. Yoshida, "The effect of ocular warming on ocular circulation in healthy humans," Arch Ophthalmol **122**, 1477-1481 (2004).

1. Introduction

Diffusing-wave-spectroscopy (DWS) is a technique able to monitor microscopic movements in turbid media. The possibility of probing the dynamics of complex fluids and tissues was previously reported [1-3]. Practically, DWS extends the utility of dynamic light scattering to strongly multiply scattering media [4]. The most fascinating feature of this technique is the ability to resolve the molecules motion, e.g. thermal motion and blood flow, in static matrix of tissue.

In this study, we report the first observation of a diffusing-wave-spectroscopy signal recorded in-vivo on the ocular fundus of a rabbit eye. The paper first discusses the theoretical approach and possible simplification (Section 2) to make possible the consideration of a complex tissue such as the ocular fundus. In Section 3, we present the experimental methods used to investigate in-vivo diffusing-wave-spectroscopy. To show the sensitivity of the method, the study was carried out analyzing the thermal effect of a low-power continuous wave infrared laser radiation on a pigmented rabbit retina. Section 4 is devoted to present the results obtained. We conclude with a discussion concerning the temperature induced vasodynamics of the choroids.

2. Measuring principle

A schematic diagram of the measuring principle is shown in Fig. 1. Ocular fundus tissue is illuminated by a laser beam. Photons migrate through the tissue and some of them are collected at distance R from the illumination point.

Absorption and scattering are the predominant phenomena governing photons propagation. Absorption effects are described by the absorption coefficient μ_a whereas scattering effects are described by the reduced scattering or transport scattering coefficient

$$\mu'_s = (1-g)\cdot\mu_s, \tag{1}$$

where μ_s is the scattering coefficient and g is the mean cosine of the scattering angle.

#77218 - $15.00 USD Received 17 November 2006; revised 17 January 2007; accepted 7 March 2007

The photon transport mean free path l^*, defined as

$$l^* = (\mu_a + \mu'_s)^{-1}, \tag{2}$$

represents the average distance between scattering or absorption events.

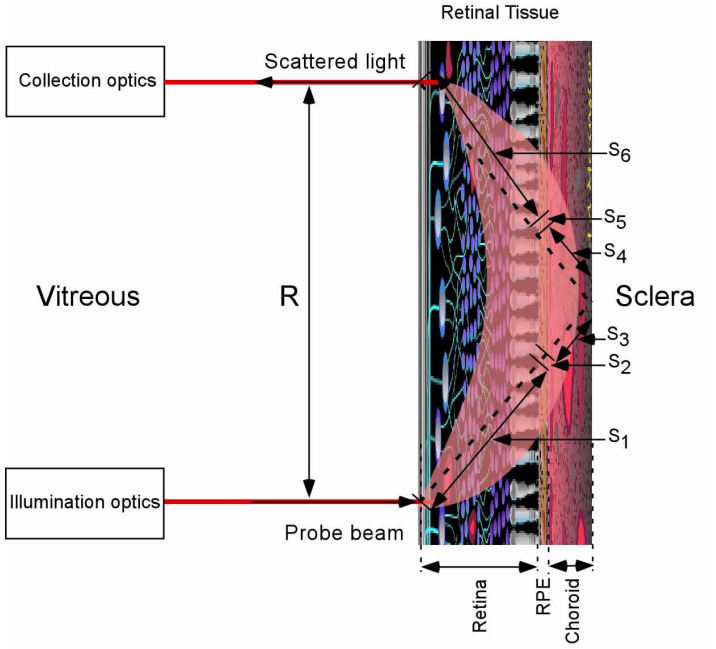

Fig. 1. Photon migration through the ocular fundus tissue. The "banana shaped" light red region represents the distribution of photons, which travel through the tissue from the illumination to the collection optics.

Ocular fundus consists of four main layers: (i) retina, (ii) retina pigment epithelium (RPE), (iii) choroids, and (iv) sclera. Table 1 reports the optical properties of bovine ocular fundus at 633 nm measured by Hammer et al. [5]. Scattering in these layers is originated by a mixture of macromolecules. Some of these molecules are rigidly fixed into the tissue structural matrix, whereas others can move. The motion of these molecules depends on various parameters, such as shape and size of the molecules, interaction among other molecules, constraints due to membranes, and so forth.

The movement of molecules in the fundus tissue induces a fluctuation of the intensity scattered light. In diffusing-wave spectroscopy, these fluctuations are measured and then analysed in terms of the electric field autocorrelation function, that, in turn, allows the determination of the dimensionless mean-squared displacement of the scattering sites defined as:

$$\rho(\tau) = k^2 \left\langle \Delta r^2(\tau) \right\rangle, \tag{3}$$

where $k=2\pi/\lambda$ is the wave number of light inside the tissue and $\left\langle \Delta r^2(\tau) \right\rangle$ is the mean-squared displacement of scattering sites after a time τ [6].

#77218 - $15.00 USD Received 17 November 2006; revised 17 January 2007; accepted 7 March 2007

Table 1. Optical properties of bovine retina at 633 nm measured by Hammer et al. [5]

Tissue	μ_a (mm^{-1})	μ_s (mm^{-1})	g	μ'_s (mm^{-1})	l^* (mm)
Retina	0.25	25.00	0.97	0.75	1.00
RPE	90.00	120.00	0.84	19.20	$9.15 \cdot 10^{-3}$
Choroids	8.00	60.00	0.94	3.60	$86.20 \cdot 10^{-3}$
Sclera	0.25	80.00	0.9	8.00	$121.21 \cdot 10^{-3}$

The normalized electric field autocorrelation function is given by a weighted average of the single-path correlation function [7] according to the photon paths probability density P(s):

$$g_1(\tau) = \int_{\Gamma} P(s) \cdot e^{-\frac{\rho(\tau)\cdot\gamma(s)}{3\cdot l^*(s)}} ds\,, \tag{4}$$

where $\mathbf{\Gamma}$ represents the space of all possible photon paths s and $\gamma(s)$ is the length of the generic curve *s*. Eq. (4) assumes that scattering events and particle motions are uncorrelated, and that $l^*(s)$ is larger than the wavelength of light λ. According to data reported in Table 1, the photon transport mean free paths in retina, RPE and choroids are larger than the layer thicknesses (few hundreds of microns in total) thus resulting in a quasi-ballistic propagation of the photons. Nevertheless, standard approach used in DWS theory, which allows to obtain reasonably accurate analytic prediction of the photon paths probability density [3], relies on the diffusion approximation to describe energy transport at large length scale, i.e. much longer than l^*. An alternative approach, suitable to describe fundus photon transport, was presented by Lemieux et al. [8] by modelling photon propagation by a telegrapher equation. However, exact solution is quite complex for multilayer tissues and to be calculated requires the exact knowledge of the boundary conditions and beam characteristics.

To extract preliminary information from the acquired autocorrelation functions, we consider a single path s_O possible for all the photons. In our rough approximation, we assume ballistic motion of the photons through retina, RPE and choroids whereas we assume the sclera to be a reflector. Thus the dashed line in Fig. 1 represents the path, named s_O, for all the photons. According to this simplification, the photon paths probability density P(s) is:

$$P(s) = \delta(s - s_o)\,, \tag{5}$$

where δ represents the unit impulse Dirac function.

According to Eq. (5) and dividing curve s_0 into six segments as shown in Fig. 1, Eq. (4) can be rewritten as:

$$g_1(\tau) = e^{-\rho(\tau)\cdot\sum_{i=1}^{6}\frac{\gamma(s_i)}{3\cdot l^*(s_i)}} = e^{-\rho(\tau)\cdot 2\sum_{i=1}^{3}\frac{\gamma(s_i)}{3\cdot l_i^*}}\,, \tag{6}$$

where the last equation is derived assuming the optical property and the scatters mobility spatially constant in each layer. $l_i^*(s_i) = l_i^*$ (i=1,…,6) represent the photon transport mean free paths of the retina (i=1,6), RPE (i=2,5) and Choroids (i=3,4) as reported in Table 1. Therefore from Eq. (6), the dimensionless mean-squared displacement of the scattering sites can be easily calculated as:

$$\rho(\tau) = -\frac{3}{2}\cdot\frac{l_1^*\cdot l_2^*\cdot l_3^*}{\gamma_1\cdot l_2^*\cdot l_3^* + \gamma_2\cdot l_1^*\cdot l_3^* + \gamma_3\cdot l_1^*\cdot l_2^*}\ln\left(g_1(\tau)\right), \tag{7}$$

#77218 - $15.00 USD Received 17 November 2006; revised 17 January 2007; accepted 7 March 2007

where curve lengths $\gamma(s_i) = \gamma_i$ (i=1,2,3) are shown in Fig. 1.

The motion of the scattering sites is mainly induced by temperature and blood flow. Temperature induced motion is typically in the form of Brownian motion, and is suitably described by the diffusion coefficient D_B of colloids [6]. On the other hand, blood flow in the choroidal capillaries, known as choriocapillaris, can be depicted as a Gaussian random flow described with mean square velocity $\langle v^2 \rangle$ [9], i.e. both the speed and direction of the molecules flow at any point in space are random variables with Gaussian distribution. Thus mean-squared displacement of the moving scatterers is:

$$\rho(\tau) = k^2 \left[\alpha \cdot (6 \cdot D_B \cdot \tau) + \beta \cdot \left(\langle v^2 \rangle \tau^2 \right) \right], \tag{8}$$

where α and β represent the probabilities that the photons are scattered by a scattering site in Brownian motion or in random flow respectively. Wave number of light inside the tissue k can be estimated assuming an average refraction index n=1.4 [10].

3. Experimental Methods

3.1 Optical setup

A picture of the developed system is reported in Fig. 2(a). We modified a commercial ophthalmic microscope (BQ900, Haag-Streit AG, Switzerland) equipped with a standard therapy laser diode (λ=810nm, Quantel Medical IRIDIS, France). A diaphragm system allowed the spot diameter of the treatment laser to be continuously variable from 800μm to 4100μm. Irradiation time and power were adjusted with a laser controller. A 70/30 beam splitter was used to couple probe beam and to collect the scattered light according to Fig. 1.

A HeNe laser beam was focused into a single-mode fiber. The light at the output of the fiber was collimated and coupled to the ophthalmic microscope 70/30 beam splitter by a gradient index (GRIN) lens. The resulting collimated beam was aligned to the microscope optics for the illumination of the treatment spot region. Collection of scattered radiation was performed by a second GRIN lens that focuses the scattered light into a second single mode fiber. To detect only the HeNe scattered light, an interference filter was fixed in front of the collection GRIN lens. The scattered light was then guided by the single mode fiber to a single photon counting module (SPCM-AQR-14-FC, Perkin-Elmer, Québec, Canada). The electrical signal from the SPCM was processed by a digital correlator (FLEX99S160B, Correlator.com, USA) to acquire the normalized intensity autocorrelation function $g_2(\tau)$.

In the perfectly single-mode case, as realized with the single-mode collection fiber, and supposing the normalized electric field autocorrelation function to be a real function, the intensity autocorrelation function can be written as [11]:

$$g_2(\tau) = 1 + \frac{h}{(1+h)^2} g_1(\tau) + \frac{1}{(1+h)^2} g_1(\tau)^2, \tag{9}$$

the heterodyne parameter h can be expressed as:

$$h = \frac{I_s}{\langle I_d \rangle} \tag{10}$$

where I_s and $\langle I_d \rangle$ represent the intensity of the scattered light originated from the static sites and the temporal average of the intensity of the light scattered by moving scatterers respectively. The use of a single-mode receiver assures perfect transverse coherence of the received scattered light and, therefore, the heterodyne parameter *h* can be determined from the initial value of the measured correlation function $g_2(\tau)$ [11].

#77218 - $15.00 USD Received 17 November 2006; revised 17 January 2007; accepted 7 March 2007

3.2 Measuring protocol

Experimental activity was devoted mainly to prove the ability of the system to detect the motion of the scattering sites in the ocular fundus layers. The experiment was performed on a pigmented rabbit fundus. The animal was anesthetized through intramuscular injection of ketamine (50 mg/kg; Ratiopharm, Ulm, Germany) and xylazine (3 mg/kg; BayerVital, Leverkusen, Germany).

The motion of the scattered sites in the right eye fundus was varied using a standard ophthalmic treatment procedure known as transpupillary thermotherapy (TTT). Using the near infrared therapy laser diode with a power settings of 200 mW, we induced a moderate temperature increase (lower than 10°C) of the retinal tissues for a long period (60 seconds). The advantage of near infrared light is its deeper chorioretinal penetration compared with visible light. In contrast with photocoagulation, one of the features of TTT is that it does not change the tissue morphology at the molecular level. Thus TTT is known as a sub-threshold procedure [12].

During the experiment, a Goldmann laser-coated contact lens was put on the rabbit cornea to make fundus observation easy by the microscope and to guide the treatment and probe laser radiation. The aiming beam of the therapy laser diode (λ=650 nm) was focused on the inferior parapapillary region as represented by the green spot in Fig. 2(b). The treated area diameter was estimated to be about 4 mm. The collection optics of the DWS system is completely described when a laser beam is coupled to the fiber from the detector side [11]. Thus to define the collection area, the APD photodiode was substituted by a HeNe laser. The red spots in Fig. 2(b) represent the illumination and the collection sites achieved. The distance R between illumination and collection spots was estimated to be about 2 mm.

Immediately before TTT, the SPCM was reconnected to the receiving fiber and three autocorrelation functions were acquired in 15 seconds. Next, we started the laser thermal treatment. During the 60-second NIR laser exposure, an autocorrelation functions was acquired each 5 seconds for a total of 12 readings. After the TTT three autocorrelation functions were acquired in 15 seconds. To exclude possible visible alteration of the tissues at the end of the treatment, an ophthalmologist observed the eye fundus.

4. Basic results and discussion

To evaluate the electric field autocorrelation functions, the eighteen intensity autocorrelation functions acquired in-vivo during the experiment were processed according to Eqs. (9) and (10). By collecting the three runs before and after the treatment, we confirmed good reproducibility of our optical measurements.

Figure 3(a) shows three examples of function $g_1(\tau)$ obtained before, after 30 seconds and at the end of the laser thermal treatment. The corresponding dimensionless mean-squared displacements of the scattering sites calculated according to Eq. (7) are reported in Fig. 3(b).

Values of distances path lengths s_i were calculated by considering the measuring geometry and the layers thickness of the rabbit fundus reported in literature [13]: retina, RPE and choroids thicknesses were set to 160 μm, 4 μm and 65 μm respectively.

Autocorrelation functions exhibit a similar trend and a common plateau in the delay time range (200μs, 1000μs). As one can see, all the curves tend to a constant value in this delay time range, and still continue to decrease for τ>1000μs. This shape of the autocorrelation function was observed by other researchers in randomly multilayer media with localized flow [14, 15]. The two-cells setup experiment proposed by Scheffold et al. [15], suggests a simple interpretation of the resulting correlation function in terms of contributions of the individual layers. Qualitatively, we can associate the long delay times information with the short trajectories of photons. In fact, photons with long trajectories are completely decorrelated at long delay times, thus their contribution to the field autocorrelation function is not significant. Photons with short trajectories consist of the few photons travelling into the retinal layer

#77218 - $15.00 USD Received 17 November 2006; revised 17 January 2007; accepted 7 March 2007

without reaching the choroidal capillaries. On the other hand, the contributions at short delay times become from all the photons but, as discussed in section 2, the number of photons reaching the sclera is dominant, thus the rate of decrease of $g_1(\tau)$ is mainly determined by mean-squared displacements of the scattering sites in the choroids. These considerations agree with the experimental results reported by G. Maret and P.E. Wolf [16] and are consistent with the theoretical predictions of S.E. Skinpetrov and R. Maynard [17].

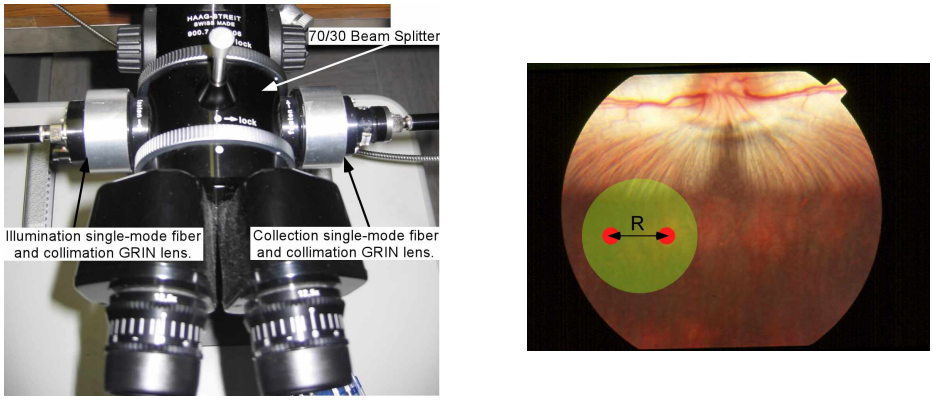

(a) (b)

Fig. 2. Picture of the modified ophthalmic microscope (a); the ophthalmic microscope, the 30/70 beam splitter and the custom made fiber adapters including the collimation lenses are shown. Pigmented rabbit fundus (b). The green spot represents the laser heated area of about 4 mm in diameter whereas the red spots correspond to the illumination and the collections sites of the DWS system.

Therefore, three different delay time intervals with different contributions from the fundus layers can be considered. The short delay range (red region in Fig. 3(b)) of the correlation function and thus of the dimensionless mean-squared displacements is bounded by the range of delay times (1μs, 100μs). The main contributions in this range become from the mean-squared displacements of the scattering sites in the choroids. In addition to scatterers in Brownian motion, the choroids contributes 85% of the ocular blood flow thus, according to Eq. (8), $\rho(\tau)$ is expected to be a quadratic function of τ. On the other hand, the long delay range (blue region in Fig. 3(b) is bounded by the range of delay times (1ms, 10ms). The main contributions in this range become from the mean-squared displacements of the scattering sites in the retina. Since the explored retina did not contain vessels, only thermal motion of scatteres is present and $\rho(\tau)$ is expected to be linear with τ. As one can see in Fig. 3(b), these expectations are confirmed by experimental observations.

The mean-squared displacements in the short and long delay range were calculated for all the acquired autocorrelation functions.

In the long delay range, we fit a linear function to $\rho(\tau)$ obtaining the slope $6 \cdot k^2 \cdot \alpha \cdot D_B$. Assuming α=1, i.e. no random flow, we evaluated the diffusion coefficient D_B of the scatterers in the retina reported in Fig. 4(a). The quality of the fitting processes was measured in terms of the correlation coefficient (Pearson's R). This parameter indicates how well the calculated curve fits the original data. This value ranges from zero to one. The closer to one, the better the fit.

For the quasi totality of the functions, the fitting correlation coefficient was close to 1. The few fittings with correlation coefficient lower than 0.98 were excluded from the analysis. The slopes estimated at the different stages of the experiment nicely show as in the retina the temperature induced a motion of the scaterers that increases monotonically during the TTT

#77218 - $15.00 USD Received 17 November 2006; revised 17 January 2007; accepted 7 March 2007

according to the exponential fitting reported in Fig. 4 (R=0.93). The time constant of about 20 seconds of the exponential fitting agrees with temperature time scale of the retina heating reported by other researchers [18]. After treatment, apparently, the diffusion coefficient of the scatterers in the retina persists its rising. Time constant and delay involved in the heating process could partially justify this point. Nevertheless, as discussed by Mainster and Reichel [19] protein conformations during TTT can be temporary or permanently changed. This fact could justify the failed baseline recovery of the diffusion coefficient.

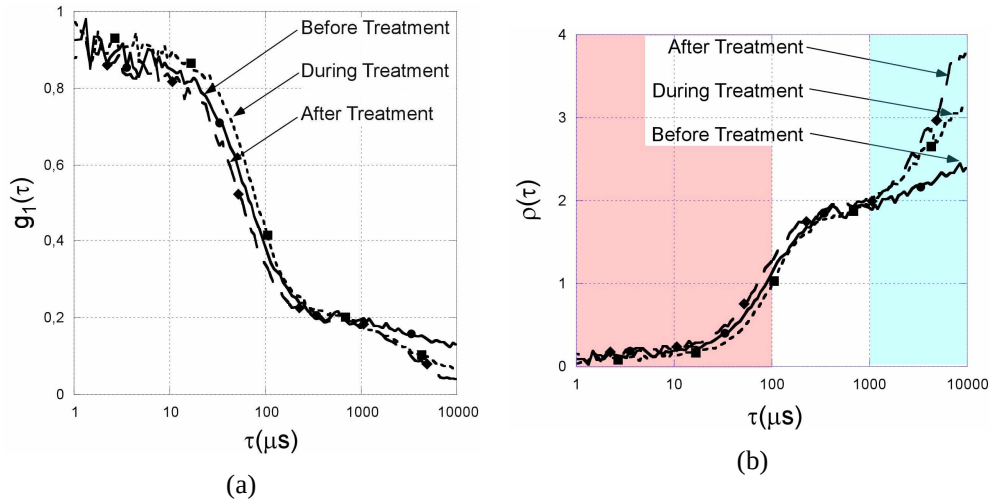

Fig. 3. Electric field autocorrelation functions obtained before (●), after 30 seconds (■) and at the end (þ) of the thermal laser treatment (a) and the corresponding dimensionless mean-squared displacements of the scattering sites (b). In the short delay range (red region) the main contribution becomes from scattering sites in the choroids whereas in the long delay range (blue region) becomes from scattering sites in the retina.

In the short delay range, we fit a quadratic function to $\rho(\tau)$ obtaining the coefficient $6 \cdot k^2 \cdot \alpha \cdot D_B$ and the blood velocity parameter $k^2 \cdot \beta \cdot \langle v^2 \rangle$ in the choroidal layer. Thus, the diffusion coefficient and the Gaussian mean square velocity were calculated including the unknown coefficients α and β as reported in Figs. 4(b) and 4(c). For the quasi totality of the functions, the fitting correlation coefficient was close to 1. The few fittings with correlation coefficient lower than 0.98 were excluded from the analysis. Experimental data reported in Figs. 4(b) and 4(c) show large variability respect to their variations. Nevertheless, choroidal diffusion coefficient exhibits a well defined trend. Surprising is the fact that this coefficient shows a very well defined, sharp step-down in response to the temperature elevation. Theoretical and experimental study showed as retina, RPE and choroidal layers after a second or two of laser exposure reach roughly the same temperature. Thus the step reduction in the diffusion coefficient does not reflect the trend of temperature but different boundary conditions or optical properties of the scatterers. As shown in Fig. 4(c), we observed as the choroidal blood velocity upon heating of the fundus slightly increased.

Temperature induced vasodynamics of choroids is known to be complex mechanism [20]. The absorption of excess light by the RPE produces heat in the outer retina which has to be dissipated if thermal damage is to be avoided. Choroidal blood flow can partially support this dissipation mechanism, however if the increase of flow corresponds to an increase of blood volume, additional optical absorption due to hemoglobin could reduce the effects of the convection heat transportation. Few studies have examined the relation between ocular temperature and choroidal blood flow [21-24]. Some researchers report the response to intense light in terms of choroidal vasodilatation and flow increasing [25]. According to these studies,

#77218 - $15.00 USD Received 17 November 2006; revised 17 January 2007; accepted 7 March 2007

vasodilation increases heat removal from the optically heated retina. However, a recent human study has shown that choroidal blood flow decreases upon heating of the eye [26]. This finding is mainly caused by the decrease in choroidal blood volume that suggests as choroidal vasculature may restrict in response to the increase in fundus temperature. This phenomenon could be confirmed by our observation in terms of reduction of the choroids diffusion coefficient. Our technique does not allow the measurement of the blood flow, thus the observed slightly increasing of the choroidal blood velocity could corresponds to a reduction of blood flow if the vasoconstriction effect is dominant.

Note as the above considerations do not take into account possible variations of the probabilities that the photons are scattered by a scattering site in Brownian motion or in random flow, i.e. parameters α and β.

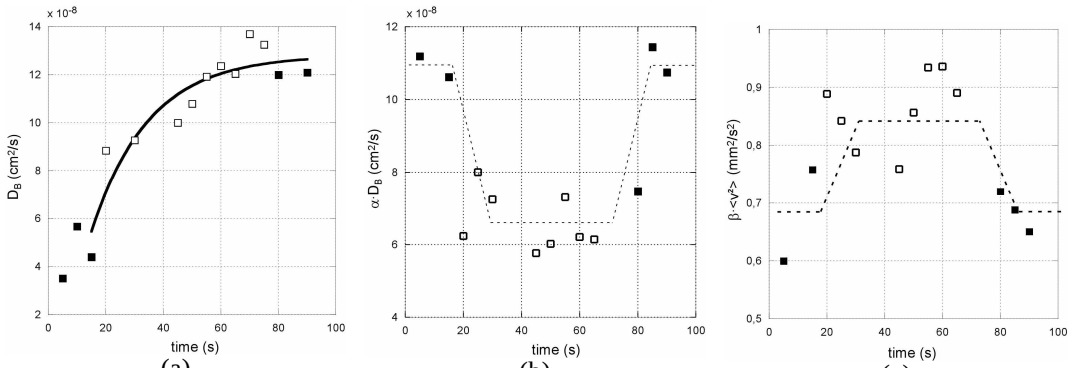

Fig. 4. Diffusion coefficient of scatterers in the retina (a), diffusion coefficient of the scatterers in the choroids (b) and Gaussian mean square velocity of the scatterers in the choroids (c). Empty squares represent the data collected during the thermal laser treatment whereas the bold squares data were collected before and after the treatment. The solid curve in (a) represents the exponential fitting to data whereas the dashed curves in (b) and (c) are guide lines for the eye through the experimental points

Acknowledgments

The authors wish to thank the Fondazione Cassa di Risparmio in Bologna and the Stella Major Foundation for their financial support to the research.

#77218 - $15.00 USD Received 17 November 2006; revised 17 January 2007; accepted 7 March 2007